Journal of Sound and Vibration 329 (2010) 2015–2028

Contents lists available at ScienceDirect

Journal of Sound and Vibration

journal homepage: www.elsevier.com/locate/jsvi

Nonlinear dynamic response and active vibration control for piezoelectric functionally graded plate

Mao Yiqi [a,b,*], Fu Yiming [a,b]

[a] State Key Laboratory of Advanced Technology of Design and Manufacturing for Vehicle Body, Hunan University, PR China
[b] College of Mechanics and Aerospace, Hunan University, Changsha 410082, China

ARTICLE INFO

Article history:
Received 20 July 2009
Received in revised form
16 December 2009
Accepted 2 January 2010
Handling Editor: L.G. Tham
Available online 22 January 2010

ABSTRACT

The nonlinear dynamic response and active vibration control of the piezoelectric functionally graded plate are analyzed in this paper. Based on higher-order shear plate theory and elastic piezoelectric theory, the nonlinear geometric and constitutive relations of the piezoelectric functionally graded plate are established, and then the nonlinear motion equations of the piezoelectric functionally graded plate are obtained through Hamilton's variational principle. The nonlinear active vibration control of the structure is carried out with adoption of the negative velocity feedback control algorithm. By applying finite difference method, the whole problem is solved by using iterative method synthetically. In numerical examples, the effects of mechanical load, electric load, the volume fraction and the geometric parameters on the dynamic response and vibration control of the piezoelectric FGM plate are investigated.

0. Introduction

A class of material known as "functionally graded material"(FGM), made such that the volume fractions of two or more materials are varied continuously along a certain dimension, has attracted much attention in many structural members and used in a wide variety of industries for its advanced properties. With the increased use of these materials, it is important to get a full comprehension of the behavior of functionally graded plates and shells. The buckling and static response of FGM composite plates and shells has been studied in literatures [1–5]. As for the dynamic properties analysis of the FGM composite plates and shells, Pradhan et al. [6] investigated the natural frequency of FGM cylindrical thin shells under various boundary conditions. Based on the high order shear deformation theory, Patel et al. [7] gave the finite element solution for the free vibration of FGM elliptical cylindrical shells. Yang [8] provided vibration characteristic and transient response of shear-deformable functionally graded plates and panels in thermal environments. There are also many investigations on the exact solutions of the FGM plates and shells [9–13].

Recently, with the development of science and technology, smart structures receive increasing wide application. The piezoelectric functionally graded plates or shells, a new sort of smart structure, are composed of piezoelectric layer imbedded or amounted on the FGM structures. The research on these new piezoelectric FGM structure increasingly becomes intense in the solid mechanics field. By exploiting its converse and direct piezoelectric effects as distributed actuators, Xiao et al. [14] investigated the performance of the functionally graded plates integrated with the piezoelectric actuators. He et al. [15] examined the active control of FGM plates with integrated piezoelectric sensors and actuators

* Corresponding author at: State Key Laboratory of Advanced Technology of Design and Manufacturing for Vehicle Body, Hunan University, PR China.
E-mail address: maoyiqi1984@163.com (M. Yiqi).

0022-460X/$ - see front matter © 2010 Elsevier Ltd. All rights reserved.
doi:10.1016/j.jsv.2010.01.005

using a finite element model. A comprehensive study was conducted for the shape and vibration control of FGM plates and shells with integrated piezoelectric sensors and actuators by Liew and coworkers using finite element method [16,17]. Satyajit et al. [18] dealt with the geometrically nonlinear dynamic analysis of functionally graded (FG) laminated composite plates integrated with a patch of active constrained layer damping (ACLD) treatment. The constraining layer of the ACLD treatment is considered to be made of the piezoelectric fiber reinforced composite (PFRC) material. Based on the first-order shear deformation theory, Ahmad et al. [19] developed an analytical solution for analysis of functionally graded material beams containing two layers of piezoelectric material used as sensors and actuator.

In this paper, based on the higher-order shear deformation theory and elastic piezoelectric theory, the nonlinear geometric and constitutive relations of the piezoelectric FGM plate are established. Assuming the distribution of electric potential along the thickness direction in the piezoelectric layer is simulated by a sinusoidal function, the nonlinear motion equations of the piezoelectric FGM plate are derived by using Hamilton's principle. An analytical model for the active vibration control of the piezoelectric FGM plate is established using the negative velocity feedback control algorithm. In the numerical examples, the effects of the volume fraction and the geometric parameters on the dynamic response and vibration control of the piezoelectric FGM plate are discussed.

1. Basic equations

Consider an orthotropic functionally graded material (FGM) plate mounted with two piezoelectric layers as shown in Fig. 1, with length a, width b, total thickness H. The rectangular Cartesian coordinate system $oxyz$ is set on the mid-plane (z=0). The bottom surface of the FGM plate is an orthotropic metal layer and the top surface is an orthotropic ceramic layer. The region between the two surfaces comprises material with different mix ratios of the ceramics and metal and can be expressed as in the following equation:

$$P_f = (1-V(z))p_m + V(z)p_c \tag{1}$$

where p_f is the effective material property of the FGM ,p_m and p_c are the properties of the metal and ceramic, respectively. $V(z)$ is the volume fraction of the metal constituent of the FGM, where z is the thickness coordinate ($-h/2 \le z \le h/2$) and h is the thickness of the FGM plate. The volume fraction is assumed to follow a power law function:

$$V(z) = (z/h + 1/2)^n \tag{2}$$

where n ($0 \le n \le \infty$) is the volume fraction index and represents the material variation profile through the plate thickness, and may be varied to obtain the optimum distribution of the constituent materials. The effective material properties of a functionally graded plate may be written as in the following equation:

$$E_f(z) = (1-V(z))E_m + V(z)E_c$$

$$\rho_f(z) = (1-V(z))\rho_m + V(z)\rho_c$$

$$v_f = \text{const.} \tag{3}$$

Reddy [20] proposed a higher-order shear deformable theory. This theory takes into account the transverse shear deformation of the structure and meets the condition that the shear force on both the bottom and top surfaces equal to zero. Based on the Reddy's higher-order shear deformation theory, the displacement field in the piezoelectric FGM plate is given by

$$u_1(x,y,z,t) = u(x,y,z) + g_1(z)\psi_1(x,y,t) - g_2(z)w_{,x}$$

$$u_2(x,y,z,t) = v(x,y,z) + g_1(z)\psi_2(x,y,t) - g_2(z)w_{,y}$$

$$u_3(x,y,z,t) = w(x,y,t) \tag{4}$$

Here, u_1, u_2, u_3 are the displacements of a point in the plate at the time t along axes x, y, z, and u, v, w are the displacements

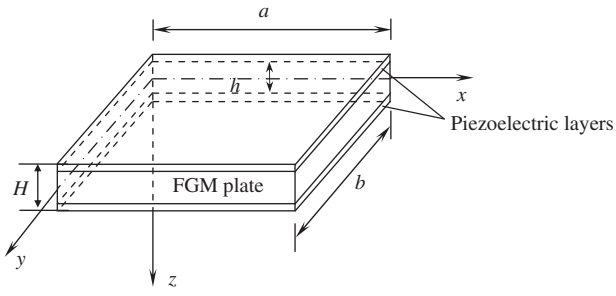

Fig. 1. Schematic diagram of the piezoelectric FGM plate.

of a point on the midplane ($z=0$) of the plate, ψ_1 and ψ_2 denote the rotations of a transverse normal about the y and x axes, respectively. The functions $g_1(z)$ and $g_2(z)$ are given as

$$g_1(z)=z\frac{4z^3}{3H^2},\quad g_2(z)=\frac{4z^3}{3H^2} \tag{5}$$

The Von Karman type geometrically nonlinear strain–displacement relations corresponding to Eq. (4) are

$$\varepsilon_x=u_{,x}+\frac{1}{2}\left(\frac{\partial w}{\partial x}\right)^2+g_1\psi_{1,x}-g_2w_{,xx}$$

$$\varepsilon_y=v_{,y}+\frac{1}{2}\left(\frac{\partial w}{\partial y}\right)^2+g_1\psi_{2,y}-g_2w_{,yy}$$

$$\varepsilon_{xy}=u_{,y}+v_{,x}+\frac{\partial w}{\partial x}\frac{\partial w}{\partial y}+g_1(\psi_{1,y}+\psi_{2,x})-2g_2w_{,xy}$$

$$\varepsilon_{xz}=g_{1,z}\psi_1-g_{2,z}w_{,x}+w_{,x}$$

$$\varepsilon_{yz}=g_{1,z}\psi_2-g_{2,z}w_{,y}+w_{,y} \tag{6}$$

The constitutive relations for an orthotropic functionally graded material are given as follows:

$$\begin{Bmatrix}\sigma_x\\ \sigma_y\\ \sigma_{xy}\end{Bmatrix}=\begin{bmatrix}c_{11}^f & c_{12}^f & 0\\ c_{21}^f & c_{22}^f & 0\\ 0 & 0 & c_{66}^f\end{bmatrix}\begin{Bmatrix}\varepsilon_x\\ \varepsilon_y\\ \varepsilon_{xy}\end{Bmatrix}$$

$$\begin{Bmatrix}\sigma_{yz}\\ \sigma_{xz}\end{Bmatrix}=\begin{bmatrix}c_{44}^f & 0\\ 0 & c_{55}^f\end{bmatrix}\begin{Bmatrix}\varepsilon_{yz}\\ \varepsilon_{xz}\end{Bmatrix} \tag{7}$$

where

$$c_{11}^f=\frac{E_1(z)}{1-v_{12}v_{21}}\quad c_{12}^f=\frac{E_2(z)v_{12}}{1-v_{12}v_{21}}\quad c_{22}^f=\frac{E_2(z)}{1-v_{12}v_{21}}$$

$$c_{44}^f=G_{13}(z)\quad c_{55}^f=G_{23}(z)\quad c_{66}^f=G_{12}(z)$$

in which, $E_1(z),E_2(z),G_{12}(z),G_{13}(z),G_{23}(z)$ represent the elastic constants varying along the thickness direction of the FGM plate and can be obtained by Eq. (1).

The constitutive relations for an orthotropic piezoelectric material is given as follows:

$$\begin{Bmatrix}\sigma_x\\ \sigma_y\\ \sigma_{xz}\\ \sigma_{yz}\\ \sigma_{xy}\end{Bmatrix}=\begin{bmatrix}c_{11}^p & c_{12}^p & 0 & 0 & 0\\ & c_{22}^p & 0 & 0 & 0\\ & & c_{44}^p & 0 & 0\\ & & & c_{55}^p & 0\\ & & & & c_{66}^p\end{bmatrix}\begin{Bmatrix}\varepsilon_x\\ \varepsilon_y\\ \varepsilon_{xz}\\ \varepsilon_{yz}\\ \varepsilon_{xy}\end{Bmatrix}-\begin{bmatrix}0 & 0 & e_{31}'\\ 0 & 0 & e_{32}'\\ 0 & e_{24} & 0\\ e_{15} & 0 & 0\\ 0 & 0 & 0\end{bmatrix}\begin{Bmatrix}E_x\\ E_y\\ E_z\end{Bmatrix}$$

$$\begin{Bmatrix}D_x\\ D_y\\ D_z\end{Bmatrix}=\begin{bmatrix}0 & 0 & 0 & e_{15} & 0\\ 0 & 0 & e_{24} & 0 & 0\\ e_{31}' & e_{32}' & 0 & 0 & 0\end{bmatrix}\begin{Bmatrix}\varepsilon_x\\ \varepsilon_y\\ \varepsilon_{xz}\\ \varepsilon_{yz}\\ \varepsilon_{xy}\end{Bmatrix}+\begin{bmatrix}g_{11} & 0 & 0\\ 0 & g_{22} & 0\\ 0 & 0 & g_{33}'\end{bmatrix}\begin{Bmatrix}E_x\\ E_y\\ E_z\end{Bmatrix} \tag{8}$$

where, D_x, D_y and D_z represent the electric displacement components; E_x, E_y, E_z denote the electric field components; $C_{ij}^p, e_{uj}', g_{ij}$ are the elastic, educed piezoelectric and dielectric permittivity constants, respectively, and

$$e_{3i}'=e_{3i}-\frac{c_{i3}e_{33}}{c_{33}}\quad (i,j=1,2),$$

$$g_{33}'=\frac{e_{33}e_{33}}{c_{33}}+g_{33} \tag{9}$$

The relations between electric field and the electric potential are

$$E_x=-\Psi_{,x}\quad E_y=-\Psi_{,y}\quad E_z=-\Psi_{,z} \tag{10}$$

For the brevity and convenience of expression, the following relations are proposed

$$x\to 1, y\to 2, z\to 3, xz\to 4, yz\to 5, xy\to 6 \tag{11}$$

Based on the Hamilton's principle, the nonlinear dynamic equations of the piezoelectric FGM plate can be derived by

$$\delta\int_{t_0}^{t_1}(K-\Pi)\,dt=0 \tag{12}$$

Here, K is the system kinetic energy, Π is the system potential energy and they can be obtained by

$$K=\int_V \tfrac{1}{2}\rho(z)\dot{u}_i\dot{u}_i\,dV$$

$$\Pi=\int_V \hbar(\varepsilon_{ij},E_i)\,dV-\int_A[q_i\dot{u}_i-Q\phi]\,dA$$

$$\hbar=\tfrac{1}{2}c_{ijkl}\varepsilon_{ij}\varepsilon_{kl}-e_{sji}E_s\varepsilon_{ij}-\tfrac{1}{2}\varepsilon_{ij}E_iE_j \tag{13}$$

where $\hbar$ is the system free energy; $\rho(z)$ is the mass density of the piezoelectric FGM plate, and for the FGM core, it can be deduced from Eq. (1), while for the piezoelectric layer, it is constant along the thickness; q_i and Q are the mechanical and electric loads applied. u_i and $\dot{u}_i$ are the displacement and velocity components, V and A denote the volume and surface area of the structure, respectively.

Employing a method similar to Ref. [21], the nonlinear dynamic equations of the piezoelectric FGM plates are obtained from Eq. (12):

$$\frac{\partial\overline{N}_1}{\partial x}+\frac{\partial\overline{N}_6}{\partial y}=I_1\ddot{u}$$

$$\frac{\partial\overline{N}_2}{\partial y}+\frac{\partial\overline{N}_6}{\partial x}=I_1\ddot{v}$$

$$\frac{\partial^2\overline{P}_1}{\partial x^2}+\frac{\partial^2\overline{P}_2}{\partial y^2}+2\frac{\partial^2\overline{P}_6}{\partial x\partial y}+\frac{\partial\overline{Q}_4}{\partial y}+\frac{\partial\overline{Q}_5}{\partial x}+q=I_1\ddot{w}$$

$$\frac{\partial\overline{M}_1}{\partial x}+\frac{\partial\overline{M}_6}{\partial y}-\overline{Q}_5=I_2\ddot{\psi}_1$$

$$\frac{\partial\overline{M}_2}{\partial y}+\frac{\partial\overline{M}_6}{\partial x}-\overline{Q}_4=I_2\ddot{\psi}_2$$

$$\int_{h/2}^{H/2}(D_{x,x}+D_{y,y}+D_{z,z}-Q_s)\,dz=0$$

$$\int_{-H/2}^{-h/2}(D_{x,x}+D_{y,y}+D_{z,z}-Q_a)\,dz=0 \tag{14}$$

Here the top piezoelectric layer is defined as the sensor, the bottom as the actuator, and the equation of motion of the sensor and actuator are presented separately as above. Q_s and Q_a are the electric load applied on the piezoelectric sensor and actuator, $(\overline{N}_i,\overline{Q}_i,\overline{M}_i,\overline{P}_i)$ are the stress resultants of the piezoelectric FGM plate, (I_1,I_2) are the mass inertia constants of the piezoelectric FGM plate. The stress resultants and inertia terms can be denoted as

$$\overline{N}_i=\int_{-H/2}^{H/2}\sigma_i\,dz,\quad \overline{M}_i=\int_{-H/2}^{H/2}\sigma_i g_1(z)\,dz,\quad \overline{P}_i=\int_{-H/2}^{H/2}\sigma_i g_2(z)\,dz\quad (i=1,2,6)$$

$$\overline{Q}_i=\int_{-H/2}^{H/2}\sigma_i g_{1,z}(z)\,dz\quad (i=4,5)$$

$$I_1=\int_{-H/2}^{H/2}\rho(z)\,dz,\quad I_2=\int_{-H/2}^{H/2}\rho(z)g_1g_1\,dz \tag{15}$$

Now, the stress resultants $(\overline{N}_i,\overline{Q}_i,\overline{M}_i,\overline{P}_i)$ are decomposed into two parts, one is that related to the piezoelectric effect, and the other related to the mechanical effect.

$$\overline{N}_i=N_i+N_i^p,\quad \overline{M}_i=M_i+M_i^p,\quad \overline{P}_i=P_i+P_i^p,\quad \overline{Q}_i=Q_i+Q_i^p \tag{16}$$

where the superscript p represents the piezoelectric effect. The component (N_i, Q_i, M_i, P_i) related to the mechanical effect can be written as

$$\begin{Bmatrix} N_1 \\ N_2 \\ N_6 \end{Bmatrix} = \begin{bmatrix} A_{11} & A_{12} & 0 \\ A_{21} & A_{22} & 0 \\ 0 & 0 & A_{66} \end{bmatrix} \begin{Bmatrix} u_{,x}+\frac{1}{2}w_{,x}^2 \\ v_{,y}+\frac{1}{2}w_{,y}^2 \\ u_{,y}+v_{,x}+w_{,x}w_{,y} \end{Bmatrix}$$

$$\begin{Bmatrix} Q_4 \\ Q_5 \end{Bmatrix} = \begin{bmatrix} F_{44} & 0 \\ 0 & F_{55} \end{bmatrix} \begin{Bmatrix} \Psi_2+w_{,y} \\ \Psi_1+w_{,x} \end{Bmatrix}$$

$$\begin{Bmatrix} M_1 \\ M_2 \\ M_6 \\ P_1 \\ P_2 \\ P_6 \end{Bmatrix} = \begin{bmatrix} B_{11} & B_{12} & & \overline{B}_{11} & \overline{B}_{12} & \\ & B_{22} & & \overline{B}_{12} & \overline{B}_{22} & \\ & & B_6 & & & \overline{B}_{66} \\ & & & D_{11} & D_{12} & \\ & & & & D_{22} & \\ & & & & & D_{66} \end{bmatrix} \begin{Bmatrix} \Psi_{1,x} \\ \Psi_{2,y} \\ \Psi_{1,y}+\Psi_{2,x} \\ -w_{,xx} \\ -w_{,yy} \\ -2w_{,xy} \end{Bmatrix} \tag{17}$$

where

$$A_{ij} = \int_{-h/2}^{h/2} c_{ij}^f(z)\,dz + \int_{h/2}^{H/2} c_{ij}^{p(s)}\,dz + \int_{-H/2}^{-h/2} c_{ij}^{p(a)}\,dz$$

$$B_{ij} = \int_{-h/2}^{h/2} c_{ij}^f(z) g_1 g_1\,dz + \int_{h/2}^{H/2} c_{ij}^{p(s)} g_1 g_1\,dz + \int_{-H/2}^{-h/2} c_{ij}^{p(a)} g_1 g_1\,dz$$

$$R_{ij} = \int_{-h/2}^{h/2} c_{ij}^f(z) g_1 g_2\,dz + \int_{h/2}^{H/2} c_{ij}^{p(s)} g_1 g_2\,dz + \int_{-H/2}^{-h/2} c_{ij}^{p(a)} g_1 g_2\,dz$$

$$D_{ij} = \int_{-h/2}^{h/2} c_{ij}^f(z) g_2 g_2\,dz + \int_{h/2}^{H/2} c_{ij}^{p(s)} g_2 g_2\,dz + \int_{-H/2}^{-h/2} c_{ij}^{p(a)} g_2 g_2\,dz$$

$$F_{44} = \int_{-h/2}^{h/2} c_{44}^f(z)\left(\frac{dg_1}{dz}\right)^2 dz + \int_{h/2}^{H/2} c_{44}^{p(s)}\left(\frac{dg_1}{dz}\right)^2 dz + \int_{-H/2}^{-h/2} c_{44}^{p(a)}\left(\frac{dg_1}{dz}\right)^2 dz$$

$$F_{55} = \int_{-h/2}^{h/2} c_{55}^f(z)\left(\frac{dg_1}{dz}\right)^2 dz + \int_{h/2}^{H/2} c_{55}^{p(s)}\left(\frac{dg_1}{dz}\right)^2 dz + \int_{-H/2}^{-h/2} c_{55}^{p(a)}\left(\frac{dg_1}{dz}\right)^2 dz$$

where c_{ij}^f are the elastic constants of FGM plate, which can be obtained from Eq. (7); $c_{ij}^{p(a)}$ and $c_{ij}^{p(s)}$ are the elastic constants of the piezoelectric sensor and actuator, respectively.

The component $(N_i^p, Q_i^p, M_i^p, P_i^p)$ related to the piezoelectric effect can be written as

$$N_1^p = \int_{-H/2}^{-h/2} (-E_z^{(a)}) e'_{31}\ dz + \int_{h/2}^{H/2} (-E_z^{(s)}) e'_{31}\ dz$$

$$N_2^p = \int_{-H/2}^{-h/2} (-E_z^{(a)}) e'_{32}\ dz + \int_{h/2}^{H/2} (-E_z^{(s)}) e'_{32}\ dz$$

$$M_1^p = \int_{-H/2}^{-h/2} (-E_z^{(a)}) g_1(z) e'_{31}\ dz + \int_{h/2}^{H/2} (-E_z^{(s)}) g_1(z) e'_{31}\ dz$$

$$M_2^p = \int_{-H/2}^{-h/2} (-E_z^{(a)}) g_1(z) e'_{32}\ dz + \int_{h/2}^{H/2} (-E_z^{(s)}) g_1(z) e'_{32}\ dz$$

$$P_1^p = \int_{-H/2}^{-h/2} (-E_z^{(a)}) g_2(z) e'_{31}\ dz + \int_{h/2}^{H/2} (-E_z^{(s)}) g_2(z) e'_{31}\ dz$$

$$P_2^p = \int_{-H/2}^{-h/2} (-E_z^{(a)}) g_2(z) e'_{32}\ dz + \int_{h/2}^{H/2} (-E_z^{(s)}) g_2(z) e'_{32}\ dz$$

$$Q_4^p = \int_{-H/2}^{-h/2} (-E_y^{(a)}) g_{1,z}(z) e_{24}\, dz + \int_{h/2}^{H/2} (-E_y^{(s)}) g_{1,z}(z) e_{24}\, dz$$

$$Q_5^p = \int_{-H/2}^{-h/2} (-E_x^{(a)}) g_{1,z}(z) e_{15}\, dz + \int_{h/2}^{H/2} (-E_x^{(s)}) g_{1,z}(z) e_{15}\, dz \tag{18}$$

where $E_i^{(a)}$ and $E_i^{(s)}$ are the electric field of the piezoelectric actuator and sensor, respectively.

In most recently published papers on piezoelectric coupled plates, the electric field is assumed constant across the thickness of the piezoelectric layer. Wang et al. [22] proved that the electrical potential distribution displays a quadratic function shape across the thickness of the beam according to Maxwell equation, and had also given a good comparison between the results obtained by the finite element analysis and the analytical results. In this paper, the distribution of the electric potential across the thickness direction of the each piezoelectric layer is assumed to be sinusoidal [22], and the electric potential at any point of the piezoelectric layer can be written as

$$\Phi(x,y,z,t) = \phi(x,y,t)\sin\left(\frac{2\pi(z-h/2)}{H-h}\right) \tag{19}$$

Introduce the following dimensionless parameters:

$$\lambda_1 = \frac{h}{a}, \quad \lambda_2 = \frac{h}{b}, \quad \lambda_3 = 1, \quad \overline{A}_{ij} = \frac{A_{ij}}{c_{11}h}, \quad \overline{B}_{ij} = \frac{B_{ij}}{c_{11}h^3}, \quad \overline{D}_{ij} = \frac{D_{ij}}{c_{11}h^3}, \quad \overline{R}_{ij} = \frac{R_{ij}}{c_{11}h^3}, \quad \overline{F}_{44} = \frac{F_{44}}{c_{11}h}$$

$$\overline{F}_{55} = \frac{F_{55}}{c_{11}h}, \quad \zeta = \frac{x}{a}, \quad \eta = \frac{y}{b}, \quad U = \frac{u}{a}, \quad V = \frac{v}{b}, \quad W = \frac{w}{h}, \quad \overline{e}_{ij} = \frac{e_{ij}}{c_{11}h}, \quad \tau = t\sqrt{\frac{E_1\lambda_1^4}{\rho_0 h^2(1-v_{12}v_{21})}}$$

$$\overline{q} = \frac{q(1-v_{12}v_{21})}{c_{11}\lambda_1^4} \tag{20}$$

Based on the previous definition of stress resultants and neglecting the in-plane inertia, the nonlinear dynamic equations of the piezoelectric FGM plate written in the form of displacements and electric field variables can be obtained by substituting Eqs. (15), (16), (17) and (18) into Eq. (14)

$$\overline{A}_{11}(U_{,\zeta\zeta} + W_{,\zeta}W_{,\zeta\zeta}) + \overline{A}_{12}(V_{,\zeta\eta} + W_{,\eta}W_{,\zeta\eta}) + \overline{A}_{66}(U_{,\eta\eta} + V_{,\zeta\eta} + W_{,\zeta\eta}W_{,\eta} + W_{,\zeta}W_{,\eta\eta}) + \frac{\partial}{\partial\zeta}\left(\int_{-H/2}^{-h/2}(-E_z^{(a)})\overline{e}_{31}dz + \int_{h/2}^{H/2}(-E_z^{(s)})\overline{e}_{31}\,dz\right) = 0 \tag{21a}$$

$$\overline{A}_{21}(U_{,\zeta\eta} + W_{,\zeta}W_{,\zeta\eta}) + \overline{A}_{22}(V_{,\eta\eta} + W_{,\eta}W_{,\eta\eta}) + \overline{A}_{66}(U_{,\zeta\eta} + V_{,\zeta\zeta} + W_{,\zeta\zeta}W_{,\eta} + W_{,\zeta}W_{,\zeta\eta}) + \frac{\partial}{\partial\eta}\left(\int_{-H/2}^{-h/2}(-E_z^{(a)})\overline{e}_{32}dz + \int_{h/2}^{H/2}(-E_z^{(s)})\overline{e}_{32}\,dz\right) = 0 \tag{21b}$$

$$\begin{aligned}&\overline{R}_{11}\Psi_{1,\zeta\zeta\zeta} + \overline{R}_{12}\Psi_{2,\zeta\zeta\eta} - \overline{D}_{11}W_{,\zeta\zeta\zeta\zeta} - \overline{D}_{12}W_{,\zeta\zeta\eta\eta} + \overline{R}_{12}\Psi_{1,\zeta\eta\eta} + \overline{R}_{22}\Psi_{2,\eta\eta\eta} - \overline{D}_{12}W_{,\zeta\zeta\eta\eta} - \overline{D}_{22}W_{,\eta\eta\eta\eta}\\ &+2\overline{B}_{66}(\Psi_{1,\zeta\eta\eta} + \Psi_{2,\zeta\zeta\eta}) - 4\overline{D}_{66}W_{,\zeta\zeta\eta\eta} + \overline{F}_{44}(W_{,\eta\eta} + \Psi_{2,\eta}) + \overline{q} + \frac{\partial}{\partial x^2}\left(\int_{-H/2}^{-h/2}(-E_z^{(a)})g_2(z)\overline{e}_{31}\,dz + \int_{h/2}^{H/2}(-E_z^{(s)})g_2(z)\overline{e}_{31}\,dz\right)\\ &+\frac{\partial}{\partial y^2}\left(\int_{-H/2}^{-h/2}(-E_z^{(a)})g_2(z)\overline{e}_{32}\,dz + \int_{h/2}^{H/2}(-E_z^{(s)})g_2(z)\overline{e}_{32}\,dz\right) + \frac{\partial}{\partial y}\left(\int_{-H/2}^{-h/2}(-E_y^{(a)})g_{1,z}(z)\overline{e}_{24}\,dz + \int_{h/2}^{H/2}(-E_y^{(s)})g_{1,z}(z)\overline{e}_{24}\,dz\right)\\ &+\frac{\partial}{\partial x}\left(\int_{-H/2}^{-h/2}(-E_x^{(a)})g_{1,z}(z)\overline{e}_{15}\,dz\right) + \int_{h/2}^{H/2}(-E_x^{(s)})g_{1,z}(z)\overline{e}_{15}\,dz) = I_1\ddot{w}\end{aligned} \tag{21c}$$

$$\begin{aligned}&\overline{B}_{11}\Psi_{1,\zeta\zeta} + \overline{B}_{12}\Psi_{2,\zeta\eta} - \overline{R}_{11}W_{,\zeta\zeta\zeta} - \overline{R}_{12}W_{,\zeta\eta\eta} + \overline{B}_{66}(\Psi_{1,\eta\eta} + \Psi_{2,\zeta\eta}) - 2\overline{R}_{66}W_{,\zeta\eta\eta} - \overline{F}_{55}(\Psi_1 + W_{,\zeta})\\ &+\frac{\partial}{\partial x}\left(\int_{-H/2}^{-h/2}(-E_z^{(a)})g_1(z)\overline{e}_{31}\,dz + \int_{h/2}^{H/2}(-E_z^{(s)})g_1(z)\overline{e}_{31}\,dz\right) - \int_{-H/2}^{-h/2}(-E_x^{(a)})g_{1,z}(z)\overline{e}_{15}\,dz - \int_{h/2}^{H/2}(-E_x^{(s)})g_{1,z}(z)\overline{e}_{15}\,dz = 0\end{aligned} \tag{21d}$$

$$\begin{aligned}&\overline{B}_{12}\Psi_{1,\zeta\eta} + \overline{B}_{22}\Psi_{2,\eta\eta} - \overline{R}_{12}W_{,\zeta\zeta\eta} - \overline{R}_{22}W_{,\eta\eta\eta} + \overline{B}_{66}(\Psi_{1,\zeta\eta} + \Psi_{2,\zeta\zeta}) - 2\overline{R}_{66}W_{,\zeta\zeta\eta} - F_{44}(\Psi_2 + W_{,\eta})\\ &+\frac{\partial}{\partial y}\left(\int_{-H/2}^{-h/2}(-E_z^{(a)})g_1(z)\overline{e}_{32}\,dz + \int_{h/2}^{H/2}(-E_z^{(s)})g_1(z)\overline{e}_{32}\,dz\right) - \int_{-H/2}^{-h/2}(-E_y^{(a)})g_{1,z}(z)\overline{e}_{24}\,dz - \int_{h/2}^{H/2}(-E_y^{(s)})g_{1,z}(z)\overline{e}_{24}\,dz = 0\end{aligned} \tag{21e}$$

$$\int_{h/2}^{H/2}(\overline{e}_{15}(g_{1,z}\Psi_{2,\zeta} - g_{2,z}W_{,\eta\zeta} + W_{,\eta\zeta}) + g_{11}E_{x,x}^{(s)} + \overline{e}_{24}(g_{1,z}\Psi_{1,\eta} - g_{2,z}W_{,\eta\zeta} + W_{,\eta\zeta}) + g_{22}E_{y,y}^{(s)} + \overline{e}_{31}(g_{1,z}\Psi_{\zeta,\zeta} - g_{2,z}W_{,\zeta\zeta})$$

$$+\bar{e}_{32}(g_{1,z}\Psi_{2,\eta}-g_{2,z}W_{,\eta\eta})+g_{33}E^{(s)}_{z,z}-Q^{ex}_{s})\,dz=0 \tag{21f}$$

$$\int_{-H/2}^{-h/2}(\bar{e}_{15}(g_{1,z}\psi_{2,\zeta}-g_{2,z}W_{,\eta\zeta}+W_{,\eta\zeta})+g_{11}E^{(a)}_{x,x}+\bar{e}_{24}(g_{1,z}\psi_{1,\eta}-g_{2,z}W_{,\eta\zeta}+W_{,\eta\zeta})+g_{22}E^{(a)}_{y,y}+\bar{e}_{31}(g_{1,z}\psi_{1,\zeta}-g_{2,z}W_{,\zeta\zeta})$$
$$+\bar{e}_{32}(g_{1,z}\psi_{2,\eta}-g_{2,z}W_{,\eta\eta})+g_{33}E^{(a)}_{z,z}-Q^{ex}_{a})\,dz=0 \tag{21g}$$

In the above equations, Q^{ex}_{s} and Q^{ex}_{a} represent the electric load applied externally on the sensor and actuator, respectively. To get a distinct presentation, the electric field $E_i(i=x,y,z)$ are not substituted by the electric potential ϕ.

Consider a piezoelectric FGM plate with four simply and immovably supported, and electrically grounded edges, so the boundary conditions are

$$\zeta=0,1:V=W=0,\Psi_2=0,N_\zeta=0,M_\zeta=0,\Phi=0$$

$$\eta=0,1:U=W=0,\Psi_1=0,\mathrm{N}_\eta=0,M_\eta=0,\Phi=0 \tag{22}$$

By integrating the FGM plate with two piezoelectric layers, sensor and actuator, to a close-loop control system, the active vibration control of the structure can be realized with the use of the negative velocity feedback control algorithm as shown in Fig. 2.

The charge output of the sensor, with poling in the z direction, can be expressed in terms of spatial integration of the electric displacement over its surface as follows:

$$Q^{(s)}(t)=\int_A D_z(t)\,dA=\tfrac{1}{2}[\int_{A(z=z_k)}D_z(t)\,dA+\int_{A(z=z_{k+1})}D_z(t)\,dA] \tag{23}$$

The current on the surface of the sensor is given by

$$I(t)=\frac{dQ^{(s)}}{dt} \tag{24}$$

The actuator voltage, to be applied on the bottom surface of the actuator, can be obtained when the current is converted into the open circuit sensor voltage and then amplified with a change of polarity as follows

$$\phi^{(a)}=-G_iG_c\frac{dQ^{(s)}}{dt} \tag{25}$$

where G_c is the constant gain of the amplifier and G_i is the gain of the amplifier to provide feedback control. Assuming the top surface of the actuator is short connected with FGM plate and the distribution of the electric potential is linear along the thickness in the actuator, the electric field in the actuator can be written as

$$E^{(a)}_z=-2\frac{G_iG_c}{H-h}\frac{dQ^{(s)}}{dt} \tag{26}$$

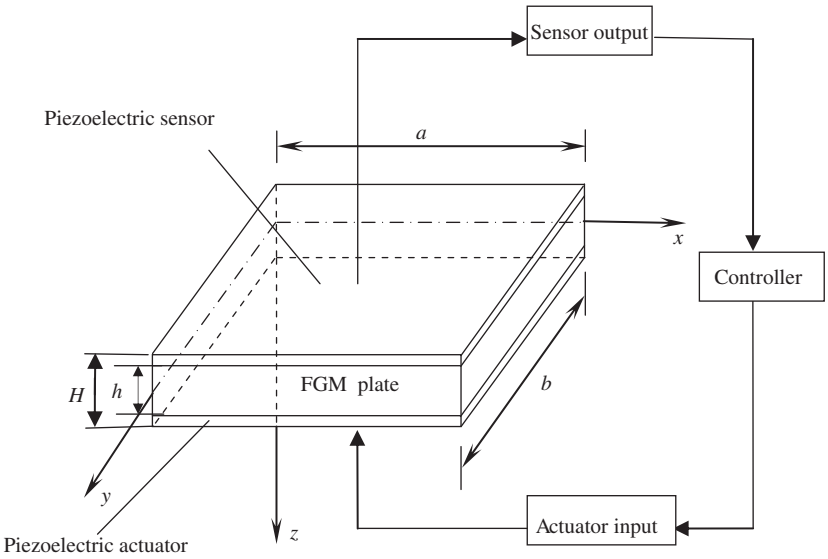

Fig. 2. Schematic diagram of the piezoelectric smart laminated plates and control loop.

2. Solution methodology

Let the piezoelectric FGM plate be subjected to a following transverse dynamic load on the top surface

$$\overline{q} = q(t)\sin\pi\xi\sin\pi\eta \tag{27}$$

In the following analysis, the $q(t)$ is set as two types as: (1) $q(t) = q_0\sin\theta\tau$, (2) $q(t) = q_0$. For the first type, the load can be considered as a sinusoidal transverse load with a fixed frequency, and the second type is a constant load.

Since the load and the structure are symmetric, only one quarter of the plate needs be considered. So the domain of the problem is selected as $0 \le \xi \le 1/2,\ 0 \le \eta \le 1/2$.

To seek the approximate solutions of the governing Eq. (21) which satisfied the boundary conditions (22), the unknown variables U, V, W and ϕ are discretized both for space and for time. The finite difference method is used for space, and the partial derivatives with respect to the space coordinate variables in the equations are replaced by difference form. The time τ is equally divided into small time segments $\Delta\tau$, and the whole equations are iterated to seek solutions. At each step of the iteration, the nonlinear items in the equations and the boundary conditions are linearized. For example, at the step J, the nonlinear items may be transformed to

$$(x\cdot y)_J = (x)_J\cdot(y)_{J_p} \tag{28}$$

where $(y)_{J_p}$ is the average value of those obtained in the preceding two iterations. For the initial step of the iteration, it can be determined by using the quadratic extrapolation, i.e.

$$(y)_{J_p} = A(y)_{J-1} + B(y)_{J-2} + C(y)_{J-3} \tag{29}$$

and for the different step of the iteration, the coefficients A, B and Ccan be expressed as follows:

$$\begin{aligned} J=1: &\quad A=1, B=0, C=0\\ J=2: &\quad A=2, B=-1, C=0\\ J\ge 3: &\quad A=3, B=-3, C=1 \end{aligned} \tag{30}$$

Moreover, using the Newmark scheme, the inertia in Eq. (21) can be expressed as follows:

$$\begin{aligned} (W_{,\tau\tau})_J &= \frac{4(W_J - W_{J-1})}{(\Delta\tau)^2} - \frac{4(W_{,\tau})_{J-1}}{\Delta\tau} - (W_{,\tau\tau})_{J-1}\\ (W_{,\tau})_J &= (W_{,\tau})_{J-1} + \tfrac{1}{2}[(W_{,\tau\tau})_{J-1} + (W_{,\tau\tau})_J]\Delta\tau \end{aligned} \tag{31}$$

The first five equations in Eq. (21) are considered when the dynamic response of the FGM plate is in discussion, and the electric field $E_z^{(a)}$ and $E_z^{(s)}$ are taken to be zero, while when the dynamic response and vibration control of the piezoelectric FGM plate are investigated, the combination of the Eqs. (8),(19) and (21) are taken to iterate for the final solutions. For every time step, the iteration lasts until the difference of the present value and the former is smaller than 0.1percent, then continue the calculation of the next step.

3. Numerical results

To ensure the validity and accuracy of the method presented in this paper, the linear free vibration of the simply supported FGM plate without consideration of piezoelectric effect was calculated. The FGM is set as aluminum–zirconia, for aluminum $E_m = 70\,\text{GPa},\ \nu_m = 0.3,\ \rho_m = 2707\,\text{kg/m}^3$, and for zirconia: $E_c = 200\,\text{GPa},\ \nu_c = 0.3,\ \rho_c = 2702\,\text{kg/m}^3$. The dimensionless fundamental frequencies $\omega(\omega = \omega_0 h^2\sqrt{\rho_m/E_m})$ are calculated and compared in Table 1 with the first-order shear deformation theory (FSDT) [24], the three-dimensional (3-D) solutions [23] and the higher-order shear-deformation solutions (HSDT) [24]. It can be observed from the Table 1 that, the FSDT over predicts the natural frequencies. When the volume fraction exponent value is set constant, the difference between the results of HSDT and FSDT becomes great as the thickness of the plate increases. Similar behavior was observed by NG et al. [25] in their prediction of origin of dynamic stability of isotropic cylindrical shell panels. It was observed in Ref. [25] that the inclusion of transverse shear stresses and

Table 1
Comparison of the dimensionless linear fundamental frequency ω for different thickness.

	n=1		h/a=0.2	
	h/a=0.05	h/a=0.2	n=2	n=5
Present	0.0160	0.2279	0.2283	0.2306
3-D [21]	0.0153	0.2192	0.2197	0.2225
HSDT [22]	0.0157	0.2257	0.2237	0.2253
FSDT [22]	0.0162	0.2323	0.2325	0.2334

rotary inertia effects in the higher-order theories generate more conservative results. However, the authors' results are a little higher than the 3-D results of Ref. [23] and results of HSDT [24], which may be due to the error from different numerical analysis and different forms of selected higher-order theory.

In the analysis of the dynamic response and active vibration control of the piezoelectric FGM plate, a ceramic-metal functionally graded rectangular plate with unmovable simply supported boundary condition is considered, and the geometric parameters are set as $\lambda 1 = \lambda 2 = 0.08$, $\lambda 3 = 1$. The following material properties are assumed in the numerical examples.

$$E_1^c = 181.0\,\text{GPa}, E_2^c = 100.3\,\text{GPa}, G_{12}^c = G_{13}^c = 50.17\,\text{GPa}, G_{23}^c = 40.87\,\text{GPa}$$

$$v_{12}^c = 0.3, \rho^c = 7800.0\,\text{Kg/m}^3$$

$$E_1^m = 106.0\,\text{GPa}, E_2^m = 10.3\,\text{GPa}, G_{12}^m = G_{13}^m = 7.17\,\text{GPa}, G_{23}^m = 3.87\,\text{GPa}$$

$$v_{12}^m = 0.28, \rho^m = 5600.0\,\text{Kg/m}^3$$

where the superscript m and c represent the metal and ceramic material, respectively.

The piezoelectric layers are chosen as PZT-5A, the material constants are

$$E_{11} = E_{22} = 61.0\,\text{GPa}, E_{33} = 53.2\,\text{GPa}, G_{12} = 22.6\,\text{GPa}, G_{13} = G_{23} = 21.1\,\text{GPa}$$

$$e_{31} = e_{32} = 7.209\,\text{C/m}^2, e_{33} = 15.118\,\text{C/m}^2, e_{24} = e_{15} = 12.72\,\text{C/m}^2, v_{12} = 0.35$$

$$\rho = 7750.0\,\text{Kg/m}^3, g_{11} = g_{22} = 1.53 \times 10^{-8}\,\text{F/m}, g_{33} = 1.5 \times 10^{-8}\,\text{F/m}$$

Fig. 3 shows the variation of the dimensionless elastic modulus of the FGM plate along the thickness direction when the volume fraction exponent value $n$is changed. The value of n equal 0 represents a fully ceramic plate, while the value of $n \to \infty$ represents a fully metal plate, and the Young's modulus changes rapidly near the bottom surface for $n = 10$.

The comparison of the linear and nonlinear dynamic response amplitude of the FGM plate when the dimensionless sinusoidal load are set as $q_0 = 5, 10, 15, 20, 25$, and θ=1 is presented in Fig. 4. The horizontal coordinate τrepresents dimensionless time, and longitudinal coordinate W_0 represents the dimensionless central deflection of the FGM plate. It can be noticed from the figure that the dimensionless deflection of the FGM plate in linear case is greater than that in nonlinear case, and this phenomenon becomes more evident when the volume fraction value n increases. Similar behavior was also observed in Ref. [26]. As we know, the linearity case is based on the limited deformation consumption, and the higher order item in the geometric relations is neglected while it is in consideration for the nonlinear case. So in some sense it can be concluded that the linear lowly predicts the stiffness of the structure. In order to reflect the dynamic property of the FGM plate accurately, the consideration of the nonlinear effect is necessary in the dynamic analysis of the structure.

Fig. 5 presents the dynamic response of the piezoelectric FGM plate and the variation of the piezoelectric potential aroused on the central surface of the piezoelectric layer. The volume fraction value is $n = 0.5$ and the frequency of the chosen sinusoidal load is θ=1. The longitudinal coordinates ϕ represents the electric potential on the central plane of the piezoelectric layer. It can be seen from the figures that the vibration amplitude and frequency of the structure as well as the sensed electric potential increases as the force increases and the sensed electric potential varies with the same frequency as the structure.

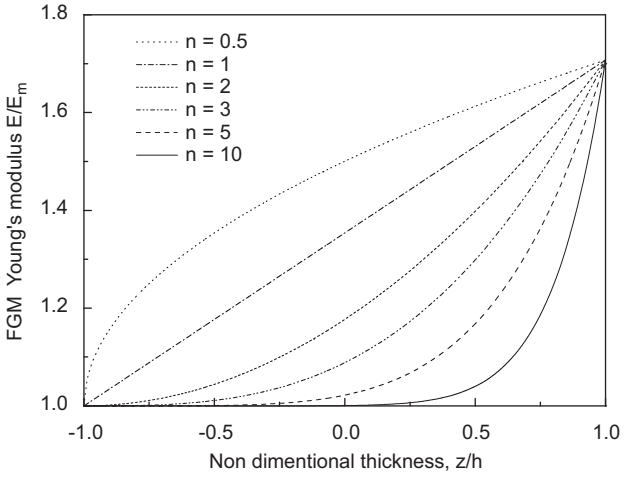

Fig. 3. Variation of Young's modulus with the non-dimensional thickness for different values of the index n.

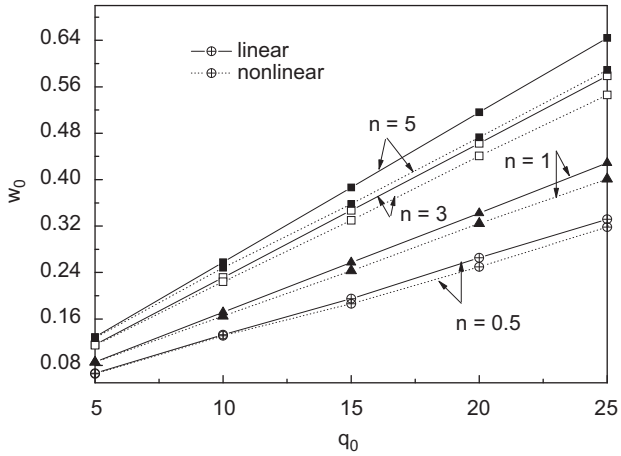

Fig. 4. Comparison of the nonlinear dynamic response amplitude of the FGM plate under different mechanical load.

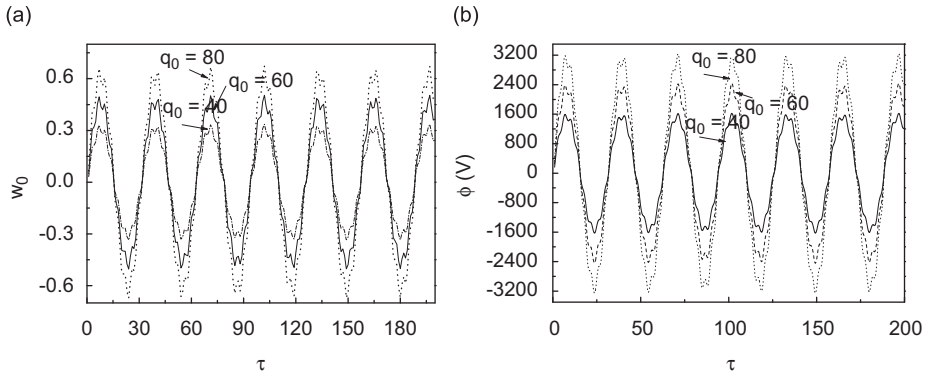

Fig. 5. Nonlinear dynamic response of the piezoelectric FGM plate and sensed voltage on the mid-plane of the piezoelectric layer.

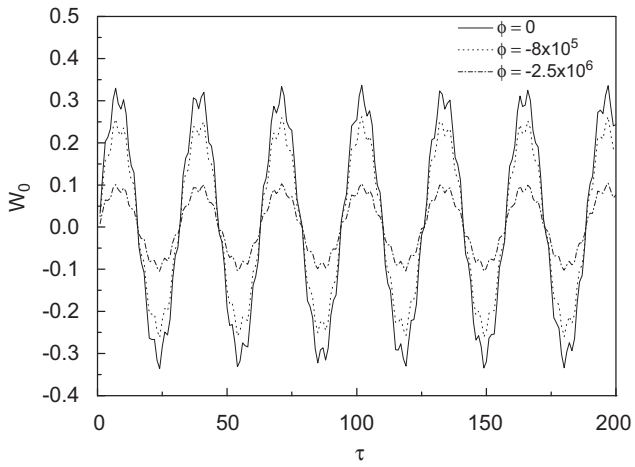

Fig. 6. Nonlinear dynamic response of the piezoelectric FGM plate under different electric load.

The effect of the electric load on the dynamic response of the FGM plate is presented in Fig. 6. The volume fraction value and the load frequency are set same as that in Fig. 5, and the mechanical load is taken as $q_0 = 40$. It can be seen from the figure that with the increase of the electric load, the nonlinear dynamic response of the structure decreases. The applied positive electric load induces a compression, and correspondingly increases the structure's stiffness, and decrease the nonlinear dynamic response amplitude of the structure.

In the Fig. 7, the effect of the volume fraction exponent value *n*on the nonlinear dynamic response of the FGM plate is discussed. The sinusoidal load is taken as, $q_0 = 30$, θ=1 in the Fig. 7(a) and a constant mechanical load is adopted in Fig. 7(b). It can be seen the deflection of the structure is comparatively small when $n = 0.2$. As the metal content in the plate increases, the stiffness of the structure decreases and the dynamic response amplitude increases. When a fixed frequency sinusoidal load is adopted, a forced vibration of the structures with the same frequency can be observed in Fig. 7(a), while in Fig. 7(b), the variation of the vibration frequency of the structure with change of the volume fraction exponent value *n* can be observed. It can be noticed when *n* is set small, high frequency of the vibration of the structures can be observed and a great effect of the *n* on the vibration frequency can be concluded. In the above Figs. 5–7(a), some nonlinear dynamic properties of the piezoelectric functionally graded plate are investigated using sinusoidal load, and high harmonics vibration of the structure can be observed. That's because more modes of the structure has been excited under this kind of load. In the following analysis, the constant mechanical load is mainly adopted.

When applying constant mechanical load on the top surface of the piezoelectric FGM plate, the effect of the thickness of the piezoelectric layer on the dynamic response of the piezoelectric FGM plates and the comparison of the dynamic response of the piezoelectric FGM plate with and without piezoelectric effect Fig. 8. Here the total thickness of the piezoelectric FGM plate is kept constant and the thickness of the piezoelectric layer and the FGM core are changed. It can be seen from the figure that the dynamic response amplitude of the piezoelectric FGM plate decreases and the vibration frequency increases when the thickness of the piezoelectric layer increases. That is due to the fact that the increase of the thickness of the piezoelectric layer would cause the increase of the stiffness of the structure. From the figure, it can also be found the dimensionless central deflection of the FGM plate decreases and the vibration frequency increases. That is because the converse piezoelectric effect causes an equivalent in-plane compressive stress, which correspondingly increase the structure's stiffness, influence the dynamic response of the FGM plate, but this effect is not so obvious.

From the previous discussion in the Fig. 6, we find that the nonlinear dynamic vibration can be depressed by exerting electric load with the use of piezoelectric layer amounted on the surface of the FGM plate. But this control should be

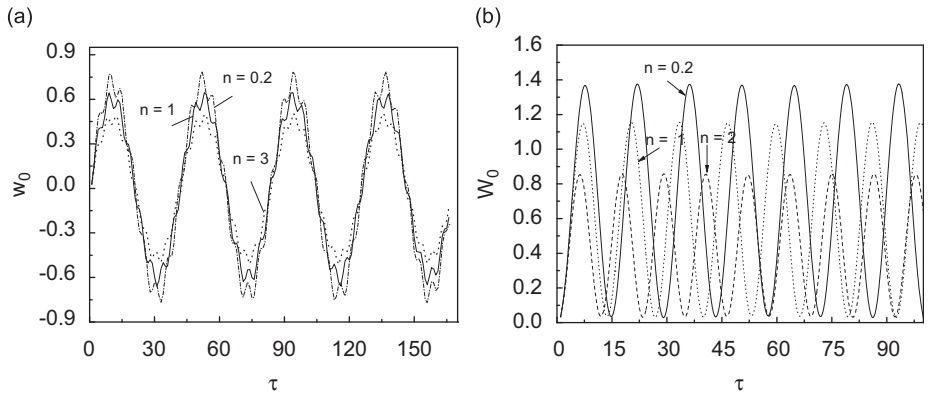

Fig. 7. Effect of the value of the volume fraction index *n* on the nonlinear dynamic response of the FGM plate.

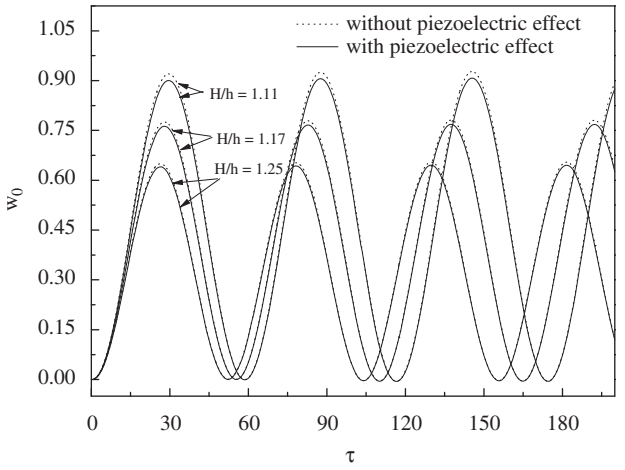

Fig. 8. Effect of the thickness of the piezoelectric layer on the nonlinear dynamic response of the piezoelectric FGM plate.

predetermined and cannot be adapted actively. With the introduction of the negative velocity feedback control algorithm, the self-adapted active control can be realized with different control goal designed. In this paper, the vibration active control is mainly discussed in the following.

We can consider the structure to work in the following manner: firstly the structure is exposed to an external constant applied mechanical load and deforms, corresponding to the deformation, generalized displacements and induced potentials in the sensors. Then the current on the surface of the piezoelectric sensor is converted into an open circuit sensor voltage which can be feed back through an amplifier to the actuator with a change of polarity. The actuator voltage produces an electric force which can be deemed as a damping in the system. During the first 10 time steps, the mechanical load (as presented in Eq. (25)) is applied on the top surface of the piezoelectric surface, and $q_0 = 100$, θ=1, the volume fraction value n=1 , the control electrical resistance is taken as $G_c = 1.0 \times 10^5$. Fig. 9 gives the effect of the control gain G_i on

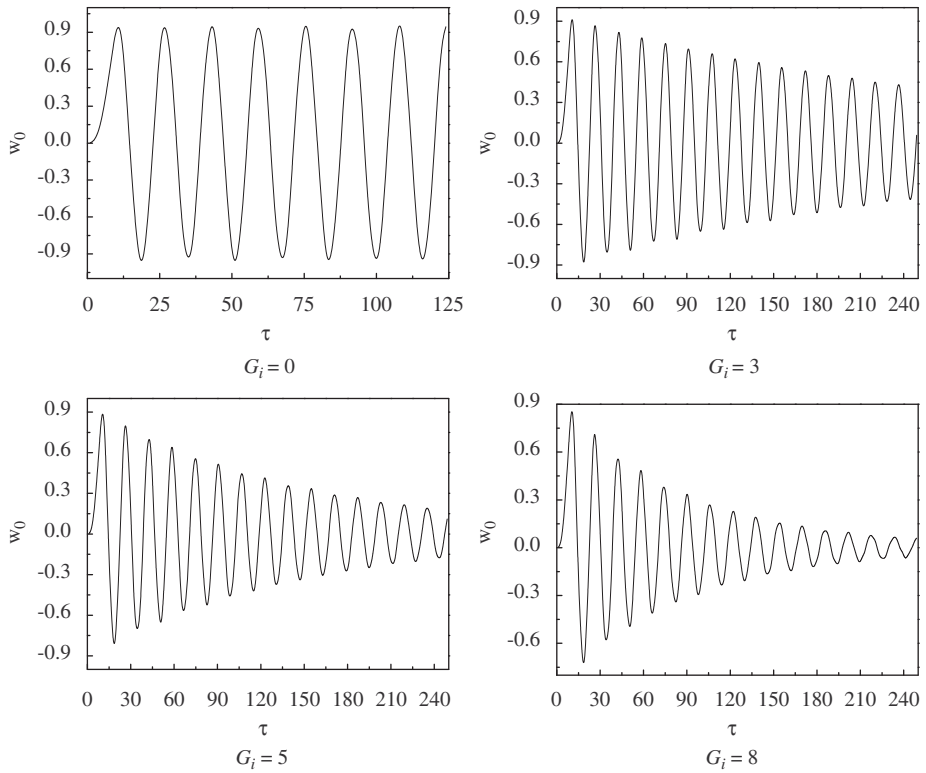

Fig. 9. Active vibration control of the piezoelectric FGM plate under different control gain G_i.

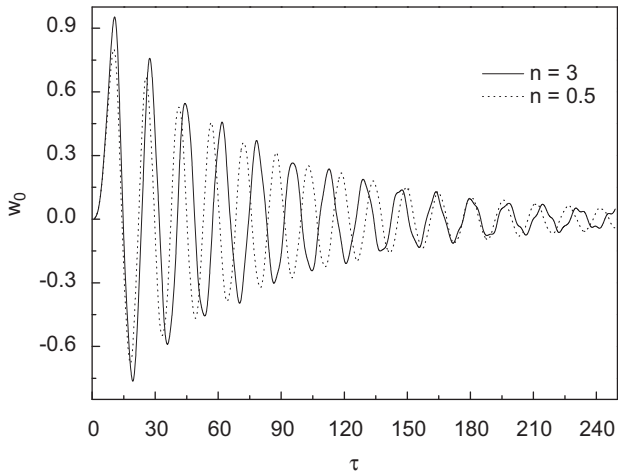

Fig. 10. Effect of the volume fraction index n on the nonlinear active vibration control of the piezoelectric FGM plate.

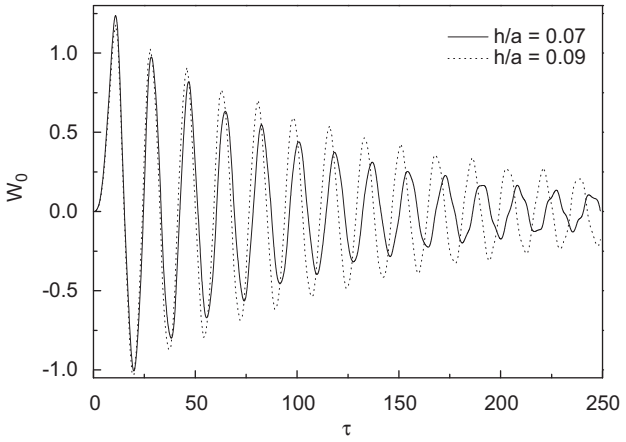

Fig. 11. Effect of the structure's geometrical parameters on the nonlinear active vibration control of the piezoelectric FGM plate.

the nonlinear dynamic response of the FGM plate. It can be seen from the figure that when control gain G_i are set as $0, 3, 5, 8$, the structure vibrate freely under the initial mechanical load. With the introduction of the control gain, an equivalent system damping is introduced, and the nonlinear dynamic response amplitude of the structure is suppressed; the bigger the control gain is, the quicker the dynamic response of the structure decreases.

The effect of the volume fraction value n on the vibration active control of the piezoelectric FGM plate is investigated in Fig. 10. The mechanical load is set as that in Fig. 9. It can be noticed from the figure that the bigger the value n is, the greater the initial dynamic response amplitude is, and the time needed to completely control the vibration is longer.

Fig. 11 shows the effect of the thickness-length ratio h/a on the central dimensionless deflection of the piezoelectric FGM plate. As reflected in Fig. 11, the decrease of the thickness-span ratio makes the vibration control of the structure more evident, that is to say, it takes a longer time to efficiently suppress the vibration of a thick piezoelastic laminated shallow spherical shell than that of a comparatively thin one.

4. Conclusion

Considering the mass and stiffness of the piezoelectric layers, the nonlinear dynamic response of the piezoelastic FGM plate with piezoelectric sensor and actuator amounted is investigated by establishing the nonlinear dynamic equations of the piezoelectric FGM plate. Using the negative velocity feedback control algorithm, an analytical model for the active control of the piezoelectric FGM plate was established. Numerical examples for orthotropic piezoelectric FGM plates are presented by using the finite element method. The main conclusions can be drawn as follows: the positive electric load produces equivalent compressive stress in the piezoelectric layer and increases the stiffness of the structure; when the volume fraction value n is larger, the initial dynamic response amplitude is greater, and the time needed to completely control the vibration is longer; the vibration control becomes more evident when the gain of amplifier G_i increases; the geometric parameters influence the vibration control of the structure to some extent.

Acknowledgment

This study is supported by the National Natural Science Foundation of China under Grant no. 10872066.

References

[1] A.H. Sofiyev, The buckling of functionally graded truncated conical shells under dynamic axial loading, *Journal of Sound and Vibration* 305 (2007) 808–826.
[2] G.N. Praveen, J.N. Reddy, Nonlinear transient thermoelastic analysis of functionally graded ceramic-metal plates, *International Journal of Solids and Structures* 35 (1998) 4457–4476.
[3] R. Kadoli, N. Ganesan, Buckling and free vibration analysis of functionally graded cylindrical shells subjected to a temperature-specified boundary condition, *Journal of Sound and Vibration* 289 (2006) 450–480.
[4] T.R. Tauchert, Thermally induced flexure buckling and vibration of plates, *Applied Mechanical Review* 44 (1991) 347–360.
[5] L.S. Ma, T.J. Wang, Nonlinear bending and post-bucking of a functionally graded circular plate under mechanical and thermal loadings, *International Journal of Solids and Structures* 40 (2003) 3311–3330.
[6] S.C. Pardhan, C.T. Loy, K.Y. Lam, J.N. Reddy, Vibration characteristics of functionally graded cylindrical shells under various boundary conditions, *Applied Acoustics* 61 (2000) 111–129.
[7] B.P. Patel, S.S. Gupat, M.S. Loknath, C.P. Kadu, Free vibration analysis of functionally graded elliptical cylindrical shells using higher-order theory, *Composite Structures* 69 (2005) 259–270.

[8] J. Yang, H.S. Shen, Free vibration and parametric resonance of shear deformable functionally graded cylindrical panels, *Journal of Sound and Vibration* 261 (2003) 871–893.
[9] M.M. Najafizadeh, H.R. Heydari, An exact solution for buckling of functionally graded circular plates based on higher order shear deformation plate theory under uniform radial compression, *International Journal of Mechanical Science* 50 (3) (2008) 603–612.
[10] P.W. Chih, S.S. Yun, Exact solutions of functionally graded piezoelectric shells under cylindrical bending, *International Journal of Solids and Structures* 44 (20) (2007) 6450–6472.
[11] H.L. Dai, Y.M. Fu, Z.M. Dong, Exact solutions for functionally graded pressure vessels in a uniform magnetic field, *International Journal of Solids and Structures* 43 (18–19) (2006) 5570–5580.
[12] Z. Shi, T. Zhang, H. Xiang, Exact solutions of heterogeneous elastic hollow cylinders, *Composite Structures* 79 (1) (2007) 140–147.
[13] P. Lu, H.P. Lee, C. Lu, Exact solutions for simply supported functionally graded piezoelectric laminates by Stroh-like formalism, *Composite Structures* 72 (3) (2006) 352–363.
[14] L.H. Xiao, H.S. Shen, Vibration and dynamic response of functionally graded plates with piezoelectric actuators in thermal environments, *Journal of Sound and Vibration* 289 (2006) 25–53.
[15] X.Q. He, T.Y. Ng, S. Sivashanker, K.M. Liew, Active control of FGM plates with integraded piezoelectric sensors and actuators, *International Journal of Solids and Structures* 38 (2001) 1641–1655.
[16] J. Yang, S. Kitipornchai, K.M. Liew, Large amplitude vibration of thermo-electro-mechanically stressed FGM laminated plates, *Computer Methods in Applied Mechanics and Engineering* 192 (2003) 3861–3885.
[17] K.M. Liew, S. Sivashanker, X.Q. He, T.Y. Ng, The modeling and design of smart structures using functionally graded materials and piezoelectrical sensor/actuator patches, *Smart Materials and Structure* 12 (2003) 647–655.
[18] S. Panda, M.C. Ray, Active control of geometrically nonlinear vibrations of functionally graded laminated composite plates using piezoelectric fiber reinforced composites, *Journal of Sound and Vibration* 325 (2009) 186–205.
[19] G. Ahmad, S. Manouchehr, F. Saeed, Deflection control of functionally graded material beams with bonded piezoelectric sensors and actuators, *Materials Science and Engineering A* 498 (2008) 110–114.
[20] J.N. Reddy, A simple higher-order theory for laminated composite plates, *Journal of Applied Mechanics* 51 (1984) 745–752.
[21] J.A. Mitchell, J.N. Reddy, A refined hybrid plate theory for composite laminates with piezoelectric laminate, *International Journal of Solids and Structures* 32 (16) (1996) 2345–2367.
[22] Q. Wang, S.T. Quek, C.T. Sun, X. Liu, Analysis of piezoelectric coupled circular plate, *Smart Materials and Structures* 10 (2001) 229–239.
[23] S.S. Vel, R.C. Batra, Three-dimensional exact solution for the vibration of functionally graded rectangular plates, *Journal of Sound and Vibration* 272 (2004) 703–730.
[24] S. Pradyumna, J.N. Bandyopadhyay, Free vibration analysis of functionally graded curved panels using a higher-order finite element formulation, *Journal of Sound and Vibration* 318 (2008) 176–192.
[25] T.Y. Ng, K.Y. Lam, J.N. Reddy, Dynamic stability of cylindrical panels with transverse shear effects, *International Journal of Solids and Structures* 36 (1999) 3483–3496.
[26] Y.M. Fu, *Nonlinear Dynamic Response Analysis of the Structure [M]*, Jinan University Press, Guangzhou, 1997.